IEEE Photonics Journal
An IEEE Photonics Society Publication

256 Gb/s Four-Channel SDM-Based PAM4 FSO-UWOC Convergent System

Volume 11, Number 2, April 2019

Wen-Shing Tsai
Chung-Yi Li
Hai-Han Lu, ***Senior Member, IEEE***
Yi-Feng Lu
Shi-Cheng Tu
Yong-Cheng Huang

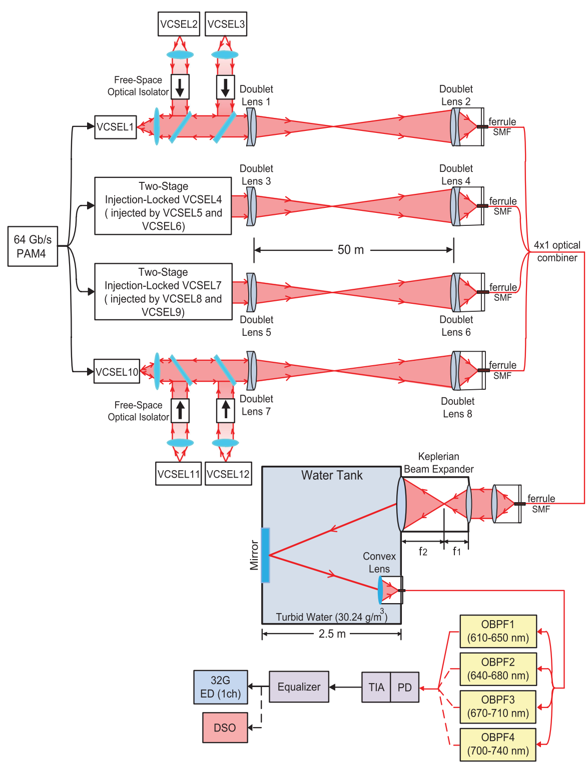

DOI: 10.1109/JPHOT.2019.2900994

256 Gb/s Four-Channel SDM-Based PAM4 FSO-UWOC Convergent System

Wen-Shing Tsai,[1] **Chung-Yi Li,**[2]
Hai-Han Lu,[3] ***Senior Member, IEEE*, Yi-Feng Lu,**[3] **Shi-Cheng Tu,**[3]
and Yong-Cheng Huang[3]

[1]Department of Electrical Engineering, Ming Chi University of Technology, New Taipei City 24301, Taiwan
[2]Department of Communication Engineering, National Taipei University, New Taipei City 23741, Taiwan
[3]Institute of Electro-Optical Engineering, National Taipei University of Technology, Taipei 10608, Taiwan

DOI:10.1109/JPHOT.2019.2900994

Manuscript received December 10, 2018; revised February 18, 2019; accepted February 19, 2019. Date of publication February 22, 2019; date of current version March 8, 2019. This work was supported by the Ministry of Science and Technology of Taiwan under Grants 106-2221-E-131-018-MY2, 107-2636-E-027-002, 107-2221-E-027-077-MY3, and 107-2221-E-027-078-MY3. Corresponding author: Hai-Han Lu (e-mail: hhlu@ntut.edu.tw).

Abstract: Given the rising demand for free-space with underwater environmental monitoring, calamity precaution, and developed industry applications, a free-space optical (FSO)–underwater wireless optical communication (UWOC) convergence is constructed to be an attractive architecture for affording a high transmission capacity. A 256-Gb/s four-channel space-division-multiplexing (SDM)-based four-level pulse-amplitude modulation (PAM4) FSO-UWOC convergent system that exploits two-stage injection-locked red-light vertical-cavity surface-emitting laser transmitters is, thus, offered and practically demonstrated. With a four-channel SDM scheme and PAM4 modulation, the total transmission capacity is drastically enhanced to 256 Gb/s. To the best of our understanding, this architecture is the leading one to build a high-speed 256 Gb/s FSO-UWOC convergent system with competent performances. It directs an approach to expedite extensive applications in the integration of high-speed free-space with underwater links.

Index Terms: Four-level pulse amplitude modulation, free-space optical, space-division-multiplexing, underwater wireless optical communication.

1. Introduction

Free-Space optical (FSO) [1]–[3] and underwater wireless optical communication (UWOC) [4]–[7] have gained increasing interests in recent years. The integration of FSO and UWOC is coming up as an attractive alternative to solve the connectivity hindrances [8], [9]. It is a promising convergent system that possesses several advantages, such as narrow laser beam size, world-wide availability with unlicensed optical spectrum, high transmission capacity, ease of construction, and the reuse of atmospheric/underwater working bandwidths. With the fast development of FSO-UWOC convergent systems, a rising demand boosts the requirement for high-speed optical wireless communications. To meet the demand of high-speed optical wireless communications, building a high-transmission-rate FSO-UWOC convergent system is required. In this work, a 256 Gb/s four-channel space-division-multiplexing (SDM)-based four-level pulse amplitude modulation (PAM4)

FSO-UWOC convergent system, which adopts two-stage injection-locked red-light vertical-cavity surface-emitting laser (VCSEL) transmitters through 50-m free-space transport with 5-m turbid underwater channel, is offered and successfully illustrated. For the first time to adopt four-channel SDM scheme in a PAM4 FSO-UWOC convergent system, the total capacity is drastically improved. Compared with non-return-to-zero (NRZ), PAM4 cuts the bandwidth for a given data rate in half. This phenomenon allows system designers to double the data rate in the channel without doubling the required bandwidth [10], [11]. As for orthogonal frequency-division multiplexing (OFDM) format, the OFDM signal should be generated and post-processed by MATLAB for bit error rate (BER) performance [12]. Whereas these off-line processes will increase the complexity of FSO-UWOC convergence. For SDM scheme, SDM takes advantage of physical separation to deliver different optical channels simultaneously. It is an effective scheme to improve the transmission capacity by increasing the number of optical channel [13]. No inter-channel interference effect exists as SDM scheme is utilized because each optical channel is independent. With four-channel SDM scheme and PAM4 modulation, the total capacity of the proposed four-channel SDM-based PAM4 FSO–UWOC convergent system is considerably increased up to eight times [4 (four-channel SDM scheme) $\times$ 2 (PAM4 modulation) = 8]. An FSO–UWOC convergent system with an aggregate channel capacity of 256 Gb/s (64 Gb/s/channel $\times$ 4 channels) is feasibly constructed.

In a turbid underwater link, the scattering coefficient is smaller at red-band than that at blue- or green-band. Red-band close to the 630–720 nm is approaching the lowest scattering through a turbid underwater channel [4]. As for the 3-dB bandwidth, red-light VCSEL has surpassed blue- and green-light laser diodes (LDs). Therefore, 630–720 nm red-light VCSEL transmitters are used in this demonstration. BER and eye diagrams have been taken as performance metrics in this FSO-UWOC convergent system. Qualified performances of BER and PAM4 eye diagrams are achieved at a 256 Gb/s operation through 50 m free-space transport with 5 m turbid underwater link.

A previous study demonstrated an adaptive water-air-water data information transfer using orbital angular momentum [8]. However, the gross bit rate of 1.08 Gbit/s is far less than the transmission capacity of 256 Gb/s employed in our demonstrated FSO–UWOC convergent system. Moreover, a 26 m/5.5 Gbps air-water optical wireless communication with an OFDM-modulated 520-nm LD was presented [9]. Nonetheless, the transmission distance and the transmission rate of 26 m and 5.5 Gbps are significantly less than the related values of 55 m and 256 Gb/s employed in this illustrated convergent system. In addition, a former research demonstrated a 10 Gb/s passive optical network (PON) with 500 Mb/s visible light communication (VLC) integrated system on the basis of Nyquist single carrier frequency domain equalization modulation [14]. Nevertheless, both the transmission rates (10 Gb/s for PON and 500 Mb/s for VLC) are greatly less than the related value of 256 Gb/s employed in such demonstrated FSO–UWOC convergence. Besides, the free-space link of 30 cm is far less than the corresponding value of 50 m adopted in this proposed convergence. Furthermore, an integrated optical wireless communication and OFDM–PON system for hybrid wired and wireless optical access with an adaptive envelope modulation technique was illustrated in another former study [15]. However, sophisticated adaptive envelope modulation technique is required. For an actual implementation of fiber–FSO convergent system, it is required to adopt a modulation technique with low complication. Our proposed 256 Gb/s four-channel SDM-based PAM4 FSO-UWOC convergent system has the characteristics of high-speed with sufficient flexibility, which is a promising one that can accelerate the implementation of FSO-UWOC convergence. To the authors' understanding, this demonstrated 256 Gb/s four-channel SDM-based PAM4 FSO–UWOC convergent system is the speediest one in the world that attainably constructs a high-speed FSO–UWOC convergence. It is superior over the prior FSO–UWOC and fiber–FSO convergent systems [8], [9] [14], [15] given its characteristics for developing high-speed optical wireless communications.

2. Experimental Setup

The structure of offered 256 Gb/s four-channel SDM-based FSO-UWOC convergent system with two-stage injection-locked red-light VCSEL transmitters through 50 m free-space transmission

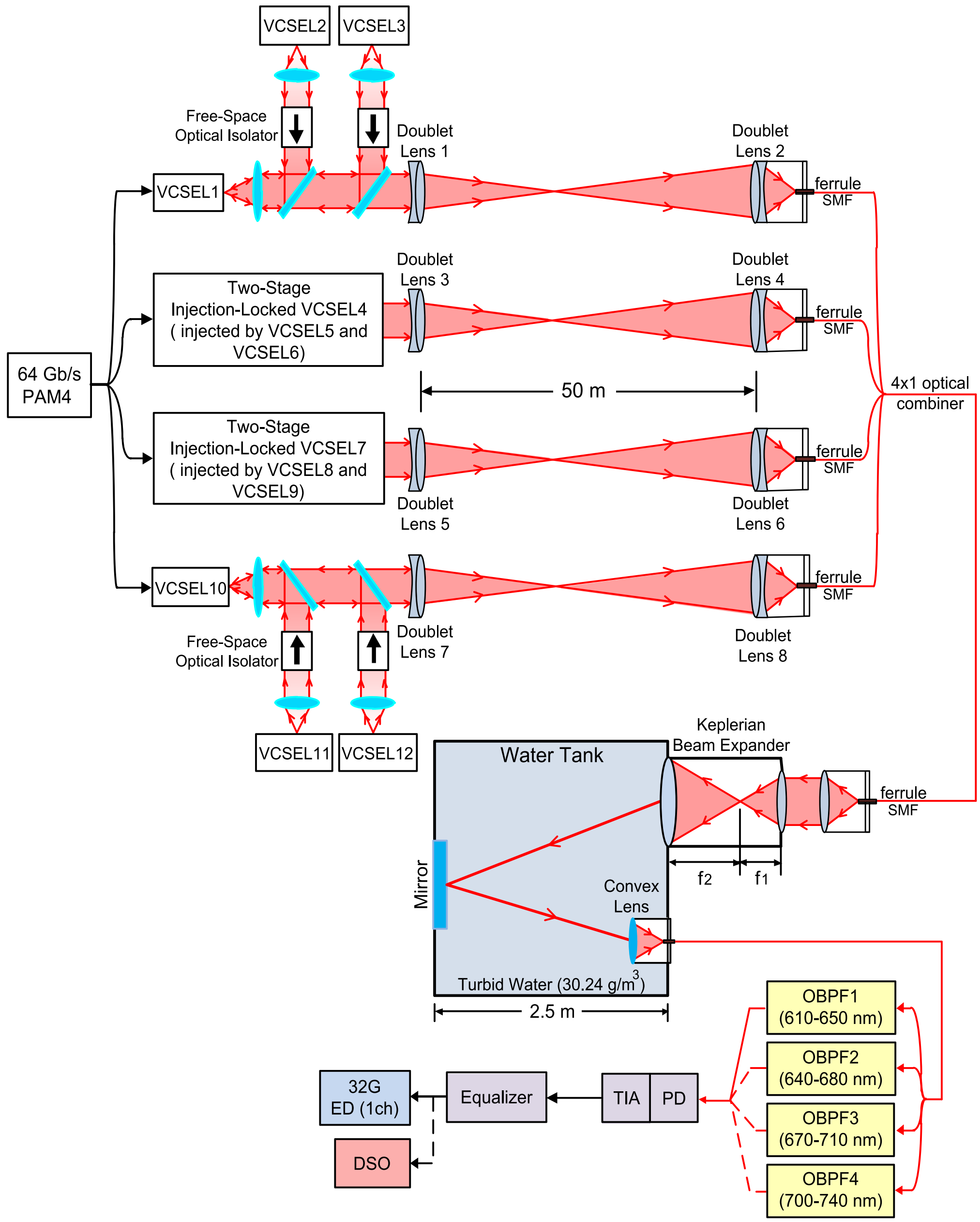

Fig. 1. The structure of offered 256 Gb/s four-channel SDM-based FSO-UWOC convergent system with two-stage injection-locked red-light VCSEL transmitters through 50 m free-space transmission with 5 m turbid underwater channel.

with 5 m turbid underwater channel is illustrated in Fig. 1. A 64 Gb/s PAM4 signal, with a pseudorandom binary sequence data stream length of $2^{15}-1$ and an amplitude of 750 mVp-p (57.5 dBmVp-p), is separated by a 1×4 RF splitter with an insertion loss of around 10 dB. VCSEL1/VCSEL4/VCSEL7/VCSEL10, with central wavelength and 3-dB bandwidth of 631.26 nm and 5.3 GHz/661.72 nm and 5.1 GHz/691.57 nm and 5.2 GHz/720.59 nm and 5.3 GHz, is directly driven by a 64 Gb/s PAM4 signal with an amplitude of 237 mVp-p (47.5 dBmVp-p). Since that PAM4 linearity is a vital factor for PAM4 VCSEL-based FSO-UWOC convergent systems, a linear driver should be deployed before the VCSEL to enhance the PAM4 signal so as to operate the VCSEL in the linear region. However, since that the power-driving current curve of VCSEL is very near the

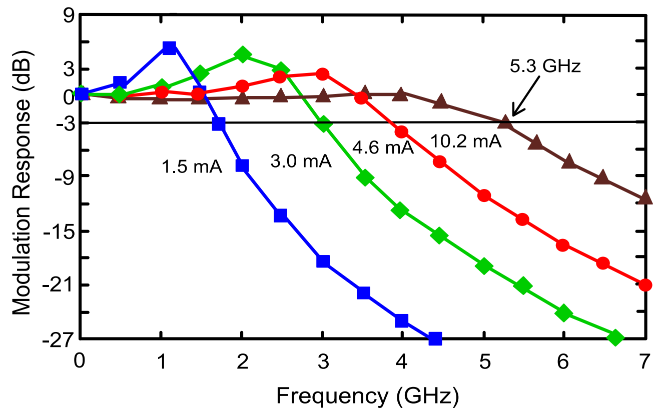

Fig. 2. The modulation response of free-running VCSEL1.

linear distribution, a linear driver to enhance the PAM4 signal is not needed. The outputs of VCSEL2 and VCSEL3 are injected into VCSEL1 via two-stage injection locking technique, designating that VCSEL2 and VCSEL3 are adopted as the first- and second-stage light injection sources (master lasers). Similarly, the outputs of VCSEL5 and VCSEL6/VCSEL8 and VCSEL9/VCSEL11 and VCSEL12 are injected into VCSEL4/VCSEL7/VCSEL10 via two-stage injection locking technique. Notably, all VCSELs (VCSEL1–VCSEL12) have similar optical features. The laser beam emitted from the two-stage injection-locked VCSEL is coupled to a 50-m free-space transmission by a set of doublet lenses. As for optical power consumption in the link, a small atmospherical attenuation of 0.4 dB exists for a 50-m free-space transmission. Since optical amplifier (erbium-doped fiber amplifier) can just boost optical signals in the region of 1550 nm, yet the optical amplifier has not been used in this convergent system. Totally, four pair of doublet lenses are deployed to construct a four-channel SDM-based FSO communication. Through a 50-m free-space transmission, four optical channels are combined by a 4 × 1 optical combiner with an aggregate channel capacity of 256 Gb/s (64 Gb/s/channel × 4-channel). Subsequently, the laser beam is sent to a Keplerian beam expander to expand the laser beam size so as to improve the underwater transmission performances [16]. Then, the expanded laser beam is delivered through a water tank with a length of 2.5 m. This water tank is full of turbid water with a particle concentration of 30.24 g/m^3. The turbidity of the underwater state is generated with suspensions of $Mg(OH)_2$ and $Al(OH)_3$, which are attained by increasing a commercial antacid preparation (Maalox) [17]. The expanded laser beam is transmitted in the turbid underwater link, reflected by a plane mirror to extend the underwater link to 5 m, focused by a convex lens, coupled into the ferrule of the optical fiber, separated by a 1 × 4 optical splitter, and traveled through four free-space optical band-pass filters (OBPFs; OBPF1–OBPF4) to select the wanted optical wavelengths. The selected optical wavelength reaches a high-bandwidth photodiode (PD) with a trans-impedance amplifier receiver to transform the optical signal into an electrical 64 Gb/s PAM4 signal. After equalization by an equalizer, we use a high-sensitivity one-channel 32 Gb/s error detector to investigate the BER performances in real-time so as to avoid the complicated post-processing by MATLAB. A digital storage oscilloscope to seize the PAM4 eye diagrams.

3. Experimental Results and Discussions

The VCSEL operates under single mode at red-light band designed for high-speed modulation, thus providing an effective way to attain competent transmission quality in high-speed optical wireless communications. The modulation response of free-running VCSEL1 is depicted in Fig. 2. Clearly, the resonance peak decreases with an increase in driving current. Given that the driving current is 10.2 mA, the 3-dB bandwidth reaches 5.3 GHz. This finding reveals that this red-light VCSEL

TABLE 1
The 3-dB Bandwidths of VCSEL1, VCSEL4, VCSEL7, and VCSEL10 for the States of Free-Running, One-Stage Injection Locking, and Two-Stage Injection Locking

VCSEL \ State	free-running	one-stage injection locking	two-stage injection locking
VCSEL1	5.3 GHz	12.2 GHz	26.3 GHz
VCSEL4	5.1 GHz	12 GHz	26 GHz
VCSEL7	5.2 GHz	12.1 GHz	26.1 GHz
VCSEL10	5.3 GHz	12.2 GHz	26.2 GHz

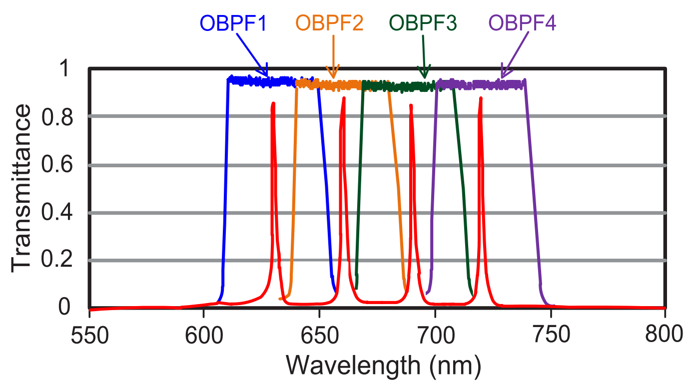

Fig. 3. The optical spectra of four separate OBPFs with passband windows of 610-650 (OBPF1), 640–680 (OBPF2), 670–710 (OBPF3), and 700–740 (OBPF4) nm; and four filtered optical wavelengths with wavelengths of 631.27, 661.73, 691.56, and 720.58 nm.

is sufficiently realized at a high-speed FSO-UWOC convergence. Moreover, the 3-dB bandwidths of VCSEL1, VCSEL4, VCSEL7, and VCSEL10 for the states of free-running, one-stage injection locking, and two-stage injection locking are given in Table 1. It is to be observed that two-stage injection locking leads to a substantial enhancement in 3-dB bandwidth [4]. By using two-stage injection locking, a considerable improvement in 3-dB bandwidth is attained. The 3-dB bandwidth can reach 26.3 GHz under the state of two-stage injection locking.

The optical spectra of four separate OBPFs with passband windows of 610–650 nm (OBPF1), 640–680 nm (OBPF2), 670–710 nm (OBPF3), and 700–740 nm (OBPF4) are presented in Fig. 3. Furthermore, the optical spectra of four filtered optical wavelengths with wavelengths of 631.27, 661.73, 691.56, and 720.58 nm are presented in Fig. 3 as well. Given the existence of a large channel spacing of 30 nm, an OBPF with a wide bandwidth of 40 nm is acceptable. Moreover, it is to be found that the optical spectrum of the VCSEL1/VCSEL4/VCSEL7/VCSEL10 moves to a slight longer wavelength (631.26/661.72/691.57/720.59 nm → 631.39/661.85/691.69/720.71 nm) as first-stage injection locking occurs, and the optical spectrum of the injection-locked VCSEL1/VCSEL4/VCSEL7/VCSEL10 moves to a slight shorter wavelength (631.39/661.85/691.69/720.71 nm → 631.27/661.73/691.56/720.58 nm) as second-stage injection locking happens. First-stage injection locking occurs when a master laser (VCSEL2/VCSEL5/VCSEL8/VCSEL11) is adjusted to a wavelength that is slightly longer than that of the slave laser (VCSEL1/VCSEL4/VCSEL7/VCSEL10). By contrast, the second-stage injection locking happens when a master laser (VCSEL3/VCSEL6/VCSEL9/VCSEL12) is adjusted to a wavelength that is slightly shorter than that of the slave laser (injection-locked VCSEL1/VCSEL4/VCSEL7/VCSEL10).

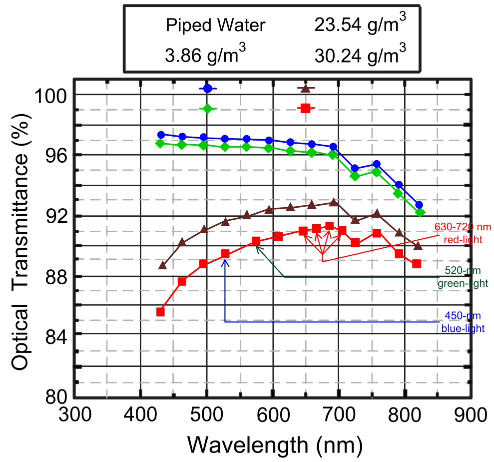

Fig. 4. The optical transmittance with particle concentrations of 0, 3.86, 23.54, and 30.24 g/m^3.

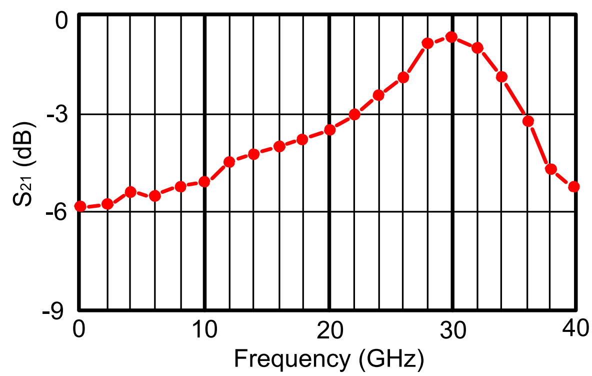

Fig. 5. The S_{21} characteristic of the linear equalizer.

The optical transmittance with particle concentrations of 0, 3.86, 23.54, and 30.24 g/m^3 are exhibited in Fig. 4. Clearly, the optical transmittance decreases with an increase in particle concentration. With particle concentrations of 0 g/m^3 (piped water) and 3.86 g/m^3 (clear ocean water), the optical transmittances of the 450-nm blue and 520-nm green wavelengths are higher than those of the 630–720 nm red wavelengths, thereby revealing the feasibility of blue- and green-light LD-based UWOC links in the piped/clear ocean underwater link. By contrast, with a particle concentration of 30.24 g/m^3 (turbid water), the optical transmittances are lower in the 450-nm blue and 520-nm green wavelengths than in the 630–720 nm red wavelengths, thus indicating the feasibility of red-light VCSEL-based UWOC links in the turbid underwater link. Conclusively, blue-light and green-light are suitable for the piped/clear ocean underwater link, whereas red-light is suitable for the turbid underwater link.

Fig. 5 shows the S_{21} characteristic of the linear equalizer. Linear equalization signifies a function intended to better the amplitudes of high frequencies compared with the amplitudes of low frequencies. In this convergence, a linear equalizer makes up for the modulation response and enhances the transmission capacity of FSO-UWOC convergent systems.

The BER performances of 64 Gb/s PAM4 signal at a selected wavelength of 631.27 nm (VCSEL1 with two-stage injection locking) for the conditions of over 50-m free-space transport (50-m FSO) and over 50-m free-space transport with 5-m turbid underwater link (55-m FSO-UWOC) are presented in Fig. 6. In addition, the BER performances of 64 Gb/s PAM4 signal at a selected wavelength of 720.58 nm (VCSEL10 with two-stage injection locking) under different conditions are shown in Fig. 7. Given that BER is 10^{-9}, there is a power penalty of 5.2 dB (see Fig. 6)/5.3 dB (see Fig. 7) between

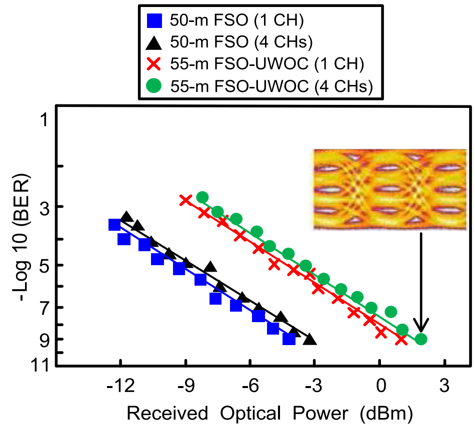

Fig. 6. The BER performances of 64 Gb/s PAM4 signal at a selected wavelength of 631.27 nm (VCSEL1 with two-stage injection locking) for the conditions of over 50-m FSO and 55-m FSO-UWOC links.

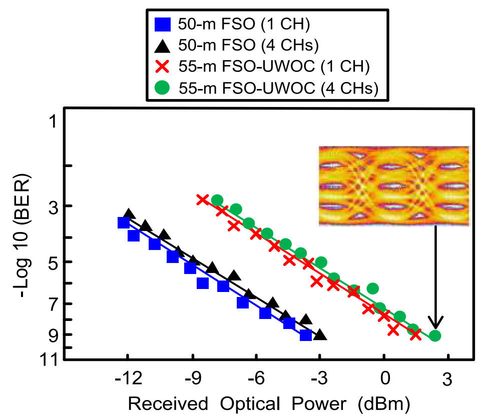

Fig. 7. The BER performances of 64 Gb/s PAM4 signal at a selected wavelength of 720.58 nm (VCSEL10 with two-stage injection locking) for the conditions of over 50-m FSO and 55-m FSO-UWOC links.

the conditions over 50-m free-space transport (50-m FSO) and over 50-m free-space transport with 5-m turbid underwater link (55-m FSO-UWOC). This 5.2 dB/5.3 dB power penalty is mainly ascribed to the optical signal-to-noise ratio (OSNR) reduction owing to additional transmission over 5 m turbid underwater link. A 5-m turbid underwater link causes scattering (attenuation) to a certain extent, in which resulting in a reduced OSNR and an increased BER. Moreover, to have a close relation with SDM scheme and BER performances, the BER performances of 64 Gb/s PAM4 signal for the scenario of only one optical channel transmission (without SDM scheme) are measured through 50-m FSO and 55-m FSO-UWOC links. Both figures (see Figs. 6 and 7) reveal that the BER values with/without four-channel SDM scheme are nearly identical, thus indicating that the interference effect for the BER performance by SDM scheme is minor. Given that each optical channel is independent, no inter-channel interference effect exists as four-channel SDM scheme is adopted. Furthermore, the eye diagrams of 64 Gb/s PAM4 signal are also displayed in Figs. 6 and 7. Evidently, qualified PAM4 eye diagrams through 50 m free-space transport with 5 m turbid underwater channel (55-m FSO-UWOC) are attained.

For the mobility issue, no mobility is provided in the FSO-UWOC line-of-sight (LOS) system even if it can provide a high-transmission-rate. As the receiver is moving around, a rapid performance decline will occur in the FSO-UWOC LOS system. However, two-dimensional steering system with blazed gratings [18] and spatial light modulator with electrical controller [19] can be deployed at the receiver side to overcome the mobility issue.

4. Conclusion

A 256 Gb/s four-channel SDM-based FSO-UWOC convergent system that uses red-light VCSEL transmitters over 50-m free-space transport with 5-m turbid underwater link is successfully constructed. Results show that four red-light VCSELs with two-stage injection locking technique are satisfactory for 256 Gb/s PAM4 signal transmission. The total transmission capacity is considerably increased by SDM scheme and PAM4 modulation. Given the aid of doublet lenses in FSO and Keplerian beam expander in UWOC, competent BER performance and qualified PAM4 eye diagrams are achieved for each optical channel. This demonstrated four-channel SDM-based FSO-UWOC convergent system is attractive for the enhancement of FSO-UWOC convergence. It possesses a promising feature for providing a high-speed optical wireless transmission and thus opens a door to expedite broad applications in the integration of high-speed free-space with underwater links.

References

[1] W. C. Wang, H. Y. Wang, and G. R. Lin, “Ultrahigh-speed violet laser diode based free-space optical communication beyond 25 Gbit/s,” *Sci. Rep.*, vol. 8, 2018, Art. no. 13142.
[2] A. Jaiswal, M. R. Bhatnagar, and V. K. Jain, “Performance evaluation of space shift keying in free-space optical communication,” *J. Opt. Commun. Netw.*, vol. 9, no. 2, pp. 149–160, 2017.
[3] W. Y. Lin *et al.*, “10 m/500 Mbps WDM visible light communication systems,” *Opt. Exp.*, vol. 20, no. 9, pp. 9919–9924, 2012.
[4] C. Y. Li *et al.*, “A 5 m/25 Gbps underwater wireless optical communication system,” *IEEE Photon. J.*, vol. 10, no. 3, Jun. 2018, Art. no. 7904809.
[5] A. Al-Halaf and B. Shihada, “UHD video transmission over bidirectional underwater wireless optical communication,” *IEEE Photon. J.*, vol. 10, no. 2, Apr. 2018, Art. no. 7902914.
[6] N. Anous, M. Abdallah, M. Uysal, and K. Qaraqe, “Performance evaluation of LOS and NLOS vertical inhomogeneous links in underwater visible light communications,” *IEEE Access*, vol. 6, pp. 22408–22420, 2018.
[7] H. Kaushal and G. Kaddoum, “Underwater optical wireless communication,” *IEEE Access*, vol. 4, pp. 1518–1547, 2016.
[8] A. Wang *et al.*, “Adaptive water-air-water data information transfer using orbital angular momentum,” *Opt. Exp.*, vol. 26, no. 7, pp. 8669–8678, 2018.
[9] Y. Chen *et al.*, “26 m/5.5 Gbps air-water optical wireless communication based on an OFDM-modulated 520-nm laser diode,” *Opt. Exp.*, vol. 25, no. 13, pp. 14760–14765, 2017.
[10] C. Y. Li *et al.*, “Real-time PAM4 fiber-IVLLC and fiber-wireless hybrid system with parallel/orthogonally polarized dual-wavelength scheme,” *OSA Continuum*, vol. 1, no. 2, pp. 320–331, 2018.
[11] G. W. Lu *et al.*, “Flexible generation of 28 Gbps PAM4 60 GHz/80 GHz radio over fiber signal by injection locking of direct multilevel modulated laser to spacing-tunable two-tone light,” *Opt. Exp.*, vol. 26, no. 16, pp. 20603–20613, 2018.
[12] C. L. Ying, H. H. Lu, C. Y. Li, C. J. Cheng, P. C. Peng, and W. J. Ho, “20-Gbps optical LiFi transport system,” *Opt. Lett.*, vol. 40, no. 14, pp. 3276–3279, 2015.
[13] C. H. Chang *et al.*, “A 100-Gbps multiple-input-multiple-output visible laser light communication system,” *IEEE/OSA J. Light. Technol.*, vol. 32, no. 24, pp. 4121–4127, Dec. 2014.
[14] Y. Wang, J. Shi, C. Yang, Y. Wang, and N. Chi, “Integrated 10 Gb/s multilevel multiband passive optical network and 500 Mb/s indoor visible light communication system based on Nyquist single carrier frequency domain equalization modulation,” *Opt. Lett.*, vol. 39, no. 9, pp. 2576–2579, 2014.
[15] C. Chen, W. D. Zhong, and D. Wu, “Integration of variable-rate OWC with OFDM-PON for hybrid optical access based on adaptive envelope modulation,” *Opt. Commun.*, vol. 381, pp. 10–17, 2016.
[16] H. M. Oubei, R. T. ElAfandy, K. H. Park, T. K. Ng, M. S. Alouini, and B. S. Ooi, “Performance evaluation of underwater wireless optical communications links in the presence of different air bubble populations,” *IEEE Photon. J.*, vol. 9, no. 2, Apr. 2017, Art. no. 7903009.
[17] M. Pittol, D. Tomacheski, D. N. Simões, V. F. Ribeiro, and R. M. C. Santana, “Evaluation of commercial $Mg(OH)_2$, $Al(OH)_3$ and TiO_2 as antimicrobial additives in thermoplastic elastomers,” *Plastics, Rubber Composites*, vol. 46, no. 5, pp. 223–230, 2017.
[18] C. W. Oh, Z. Cao, K. A. Mekonnen, E. Tangdiongga, and A. M. J. Koonen, “Low-crosstalk full-duplex all-optical indoor wireless transmission with carrier recovery,” *IEEE Photon. Lett.*, vol. 29, no. 6, pp. 539–542, Mar. 2017.
[19] Y. P. Lin *et al.*, “A 10-Gbps optical WiMAX transport system,” *Opt. Exp.*, vol. 22, no. 3, pp. 2761–2769, 2014.